High spin states and isomers in ^{151}Dy

C. J. Lister
Brookhaven National Laboratory, Upton, New York 11973

G. R. Young
Physics Division, Oak Ridge National Laboratory, Oak Ridge, Tennessee 37830
and Laboratory for Nuclear Science, Massachusetts Institute of Technology, Cambridge, Massachusetts 02139

D. Cline, J. Srebrny,* and D. Elmore
Nuclear Structure Research Laboratory, University of Rochester, Rochester, New York 14627

P. A. Butler,† R. Ledoux, and R. Fridieu
Laboratory for Nuclear Science, Massachusetts Institute of Technology, Cambridge, Massachusetts 02139
(Received 11 April 1979)

High spin states and isomers in ^{151}Dy have been studied using the ^{122}Sn(^{32}S,3n)^{151}Dy and ^{141}Pr(^{14}N,4n)^{151}Dy reactions. Levels up to $J = 53/2$ have been assigned, and two isomers at 4904 keV ($J = 41/2$, $\tau_{1/2} = 7 \pm 2$ ns) and 6032 keV ($J = 49/2$, $\tau_{1/2} = 10.9 \pm 0.6$ ns) have been identified. Gamma transitions de-exciting the isomers have $B(E2)$ values characteristic of single-particle transitions. The yrast sequence exhibits an irregular dependence on excitation energy characteristic of an independent particle model rather than a deformed rotor. In addition, above $J = 25/2$ it exhibits an effective moment of inertia of 138 MeV^{-1} which is 1.18 times the rigid sphere value. These data are compared to recent spherical and deformed shell model predictions and a qualitative agreement is found between experiment and calculation.

[NUCLEAR REACTIONS ^{122}Sn(^{32}S,3n) ^{151}Dy, E=115–165 MeV; ^{141}Pr(^{14}N, 4n) ^{151}Dy, E=60–101 MeV. Measured $\sigma(E)$, $I(\theta)$, γ-γ coinc. with pulsed beam. Deduced levels, branching ratios, spin assignments, lifetimes. Enriched targets, Ge(Li) detectors. Comparison with spherical and oblate spheroidal model calculations.]

I. INTRODUCTION

The use of γ-ray spectroscopy to study the properties of levels on or near the yrast line has been rich in revealing new nuclear phenomena. Bohr and Mottelson[1] suggested that at high angular momenta individual nucleons would align along the rotational symmetry axis producing rotational motion distinctly different from the well-known collective rotational motion. With such alignment, the individual nucleons each contribute a definite angular momentum in the direction of the rotation axis, and there are no simple generic relations between the structure of adjacent spin states in the yrast sequence. The yrast line would become irregular, the possibility of very high spin isomers would arise, and γ decays would reflect the few-nucleon nature of the states rather than the strongly enhanced $E2$ transitions characteristic of collective rotational bands.

A search for delayed high multiplicity γ decays which would be associated with the decay of such isomers was made by Pederson *et al.*[2] This survey covered many nuclei in the region $68 < N < 118$ and revealed an island of isomers in neutron deficient nuclei with $82 < N < 88$. The survey did not identify individual final nuclei or elucidate the properties of any of the isomers, but encouraged the detailed investigation of this region using conventional γ-ray spectroscopic techniques. Khoo *et al.*,[3] in an extension of earlier work,[4] investigated high spin levels in ^{152}Dy and found isomers with spins $J \approx 17$, 21, 27, and 31, while Hass *et al.*[5] have measured linear polarizations and lifetimes of levels in ^{152}Dy to establish the multipolarities and decay strengths of transitions up to spin $J \approx 36$. Similar studies have been reported by Merdinger *et al.*[6]

The research on ^{151}Dy reported in this paper was carried out in two parts: a delayed γ-γ coincidence experiment following the ^{122}Sn(^{32}S, 3n) ^{151}Dy reaction to search for isomers and establish the discrete γ-ray lines associated with their decay, followed by a series of experiments using the ^{141}Pr(^{14}N, 4n)^{151}Dy reaction to establish the detailed structure of the decay and to search for levels at higher excitation than the isomeric states.

At the onset of this work, information on ^{151}Dy was limited to the assignment[7] of a $J^{\pi} = \frac{9}{2}^{-}$ ex-

cited state at 527 keV which had been observed in the β^+ decay of ^{151}Ho. However, in addition to the present work initially reported in Ref. 8, three other groups have reported studies of in-beam spectroscopy of ^{151}Dy. A Notre Dame group[9] studied the lower spin states $J \leq \frac{25}{2}$, while a group from Jülich[10] and an Argonne-Chalk River collaboration[11] made measurements similar to the ones reported here.

The following section contains details of the experimental technique used in this work, followed by a presentation of the results. The next section contains a discussion on the interpretation of the results and some conclusions.

II. EXPERIMENTAL METHOD

A. The ^{122}Sn(^{32}S, 3n)^{151}Dy reaction

The initial study of the decay of isomers formed in the ^{122}Sn + ^{32}S reaction was done at the University of Rochester MP tandem facility using the apparatus illustrated in Fig. 1. A self-supporting target of ^{122}Sn, thickness 3 mg/cm^2, was bombarded by a ^{32}S beam at energies from 115 to 165 MeV. The experiment used a continuous beam technique in which the prompt γ rays from very highly excited states above any isomers, and consequently emitted before the nuclei left the target, were detected in either of two 7.6 × 7.6-cm NaI(Tl) detectors situated close to the target. The isomers were identified using these tag NaI detectors to define the time of formation rather than a more complex pulsed beam technique. The evaporation residues recoiled down a 19.7-cm flight tube before being stopped on a 10 mg/cm^2 ^{208}Pb catcher foil which subtended 64 mrad at the target. The catcher had a central hole subtending 30 mrad to allow passage of non-interacting beam particles to a shielded Faraday cup. The subsequent γ decay of excited nuclei captured by the catcher was observed by two Ge(Li) detectors (of 7 and 13% efficiency and 2–3-keV resolution for 1332-keV γ rays) placed ~2.5 cm from the catcher foil. These detectors were carefully shielded from direct radiation from the target by a 15-cm thick wall of tungsten plus an additional tungsten collimator which together caused a suppression of the direct radiation by a factor of $\geq 10^{+5}$ for 1-MeV γ rays.

Singles and coincidence data were recorded on-line for the Ge(Li) detectors together with time spectra between the two Ge(Li) detectors and also between one Ge(Li) detector and the NaI(Tl) tag detectors. A time resolution of 5 ns was obtained, allowing the detection of isomers with half-lives from ~5 ns to 2 μs, although the recoil flight time to the catcher of 33 ns reduced

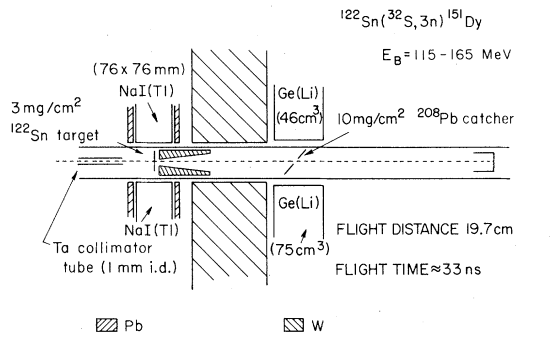

FIG. 1. The experimental apparatus used in the Rochester isomer search. The NaI(Tl) counters near the target detect prompt radiation which was used to generate "time of formation" signals. The Ge(Li) detectors downstream are shielded from prompt radiation and measure delayed radiation emitted from nuclei which have recoiled onto the Pb catcher foil.

the efficiency for the observation of short-lived isomers. For each coincidence event the two Ge(Li) energies and two timing signals were recorded event by event on magnetic tape for later analysis.

B. The ^{141}Pr(^{14}N, 4n)^{151}Dy reaction

The ^{32}S + ^{122}Sn data clearly demonstrated the existence of high spin isomers in ^{151}Dy. In addition, these data showed that the decay scheme was complicated. Therefore the ^{141}Pr(^{14}N, 4n)^{151}Dy reaction was used to study in detail the properties of the isomers and γ-decay scheme for the high spin yrast states in ^{151}Dy. In these experiments a 1.7-mg/cm^2 ^{141}Pr target evaporated onto a 3-mg/cm^2 Ta backing was bombarded with 60 to 101-MeV ^{14}N ions provided by the Brookhaven National Laboratory MP-7 tandem Van de Graaff accelerator. γ rays were detected using two Ge(Li) detectors of 13% efficiency and energy resolution of 2.1 keV for 1332-keV radiation. An excitation function was measured for γ-ray lines excited in the ^{141}Pr(^{14}N, $x n$)$^{155-x}$Dy reaction. The discrete lines previously observed in the ^{122}Sn + ^{32}S reaction were seen, together with γ rays known to be associated with ^{152}Dy (at lower bombarding energies) and with ^{150}Dy (at higher energies).[12]

Angular distributions of γ rays and prompt γ-γ coincidences were measured simultaneously at a bombarding energy of $E(^{14}\text{N}) = 75$ MeV, where the relative yield of ^{151}Dy γ radiation was the strongest. The detectors were mounted on an automatic goniometer at a distance of 10 cm from the target. One detector cycled over angles in the range 25°–100° (relative to the beam direc-

tion) while the other counter remained fixed at 270° to serve as a monitor. Prompt γ-ray coincidences between the two detectors were recorded simultaneously and were stored on magnetic tape.

Finally, a pulsed ^{14}N beam of 80 MeV was used to measure the half-lives of the isomers and to attempt to locate levels lying above them. A smaller target chamber was used allowing the γ detectors to be placed 5 cm from the target and perpendicular to the beam direction. The beam pulsing system had a repetition rate of 4 MHz and a time resolution of 8 ns was obtained for prompt γ radiation observed with the Ge(Li) detectors. Five parameter data were recorded, including the pulse height spectra from the two Ge(Li) detectors, together with the times of the γ signals relative to the beam and to each other.

C. Analysis of data

Off-line analysis of the data was done using both the peak fitting program SAMPO[13] and a fitting routine employing an interaction display unit. The yield curve data were normalized to the integrated beam, while the angular distribution data were normalized to the strong 344-keV line in the monitor detector. Both normalizations were checked for consistency by observing a smooth behavior of the 41-keV Kα x ray of praseodymium. The angular distribution data were fitted to an expansion of even Legendre polynomials:

$$W(\theta) = A_0[1 + a_2 P_2(\cos\theta) + a_4 P_4(\cos\theta)] .$$

The absolute intensities A_0 were used in the calculation of branching ratios and in the construction of the decay scheme. The coefficients a_2 and a_4 were used as a basis for assigning level spins.

The ^{141}Pr + ^{14}N reaction coincidence data from the 75-MeV run were sorted with a 20-ns wide time window and the Compton background and time randoms were subtracted. The data from the 80-MeV pulsed beam experiment were sorted to obtain background subtracted time spectra in coincidence with each γ ray. In addition, these data were sorted to search for events involving a delayed γ ray in one detector (delayed by more than 10 and less than 50 ns after the beam pulse) which had a corresponding prompt (within 10 ns of the beam pulse) event in the other detector. This method of analysis gave a strong enhancement to γ rays lying above the isomers.

III. RESULTS

A. The ^{122}Sn(^{32}S, 3n)^{151}Dy reaction

A spectrum of delayed coincident γ rays is shown in Fig. 2(a). This spectrum is formed by taking coincidences between the Ge(Li) de-

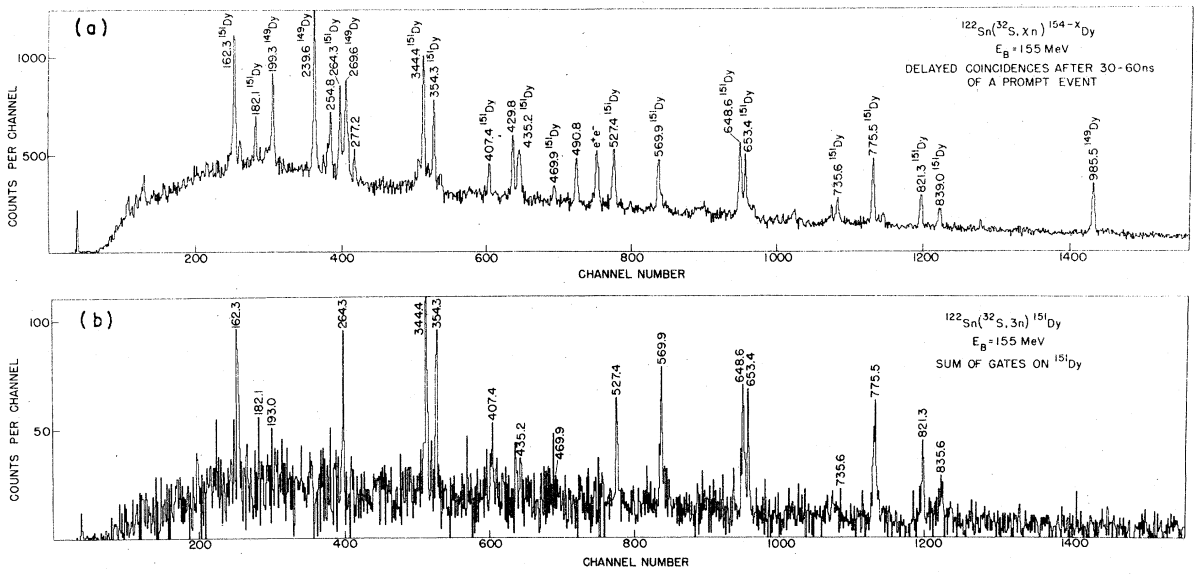

FIG. 2. Delayed γ-ray spectra following the ^{122}Sn + ^{32}S reaction at 150 MeV. Figure 2(a) is a spectrum of all γ decays from the ^{208}Pb catcher foil occurring between 30–60 ns after a prompt event detected in one of the NaI(Tl) tag counters. Figure 2(b) shows a spectrum formed from the sum of gates set on low-lying transitions in ^{151}Dy during the delayed γ-γ part of this experiment.

tectors which occurred 30–60 ns after a prompt NaI trigger signal. Transitions belonging to the decay of the 2661-keV isomer[14] in ^{149}Dy were identified, together with a cascade of γ rays which had not been previously reported. In Fig. 2(b) a spectrum is illustrated which is formed from the sum of spectra which have windows set on several of these latter transitions. It can be seen that there are large variations in γ-ray intensity which indicates that the γ cascade is not simple but exhibits forking. One of the strongest γ transitions had a transition energy of 527.4 ± 0.1 keV which indicated that this new cascade of γ rays occurred in ^{151}Dy since a 527.4± 0.1-MeV transition has been reported[7] for the $\frac{9}{2}^-$ to $\frac{7}{2}^-$ ground state transition following the β^+ decay of ^{151}Ho. The excitation functions for known low-lying transitions in ^{149,150}Dy and the new cascade of γ rays observed with the ^{122}Sn + ^{32}S reaction indicated that the new isomers occurred in ^{151}Dy. The yield of the ^{151}Dy isomers peaked at a ^{32}S bombarding energy of 145 MeV.

Table I summarizes the γ transitions observed with the ^{122}Sn(^{32}S, 3n)^{151}Dy reaction. The intensities are corrected for internal conversion[15] using the γ multipolarities derived from the ^{141}Pr(^{14}N, 4n) reaction data (see Table II). These intensities agree with the decay scheme illustrated in Fig. 3 for the 6032.1-keV and 4903.9-keV isomers. An analysis of the time spectra of several of the low-lying transitions yielded an apparent half-life measurement of $\tau_{1/2}$ = 15.5 ± 1.5 ns. However, this results from feeding through two isomers (see Fig. 3). The decay curves of the 264.3-keV and 839.0-keV transitions gave a half-life of $\tau_{1/2}$ = 11 ± 6 ns, indicating the possibility of more than one isomer. This was confirmed in the ^{141}Pr + ^{14}N measurements.

B. The ^{141}Pr(^{14}N, 4n)^{151}Dy reaction

The yield curves for known low-lying transitions in ^{150,152}Dy are illustrated in Fig. 4, together with some of the γ rays associated with ^{151}Dy. It can be seen that the ^{141}Pr(^{14}N, 3n)^{152}Dy reaction channel is strongest at 60 MeV, but the 4n and 5n evaporation channels become dominant at higher beam energies. A computation of

TABLE I. A comparison of relative yields of γ rays observed in ^{151}Dy formed in the ^{141}Pr(^{14}N, 4n)^{151}Dy and ^{122}Sn(^{32}S, 3n)^{151}Dy reactions. The former data have a mean error of ± 2%, the latter ± 10%.

	Intensity		
E_γ (keV)	^{141}Pr(^{14}N, 4n)^{151}Dy in beam[a]	^{141}Pr(^{14}N, 4n)^{151}Dy isomer decay[b]	^{122}Sn(^{32}S, 3n)^{151}Dy isomer decay[c]
527.4	74	68	68
821.3	74	74	76
573.5	5	6	*C*
569.9	68	74	63
775.5[d]	33	32	*x*
193.0	3	3	3
735.6	29	29	23
542.5	3	3	*W*
407.4	32	32	22
344.4	100	100	93
648.6	99	100	100
775.4[d]	78	92	(93 − *x*)
653.4	65	78	68
572.5	7	12	*C*
354.3	48	82	72
469.9	16	4	*C*
877.8	3	4	*W*
435.2	11	18	*C*
162.3	59	100	73
839.0	32	100	51
264.3	25	100	52

[a] Intensities from 75-MeV data.

[b] These data are derived assuming 100% population of the 6032-keV isomer and following the decay paths defined by the branching ratios in Table II.

[c] Intensities from 150-MeV data 30–60 ns after a prompt trigger signal.

[d] Doublet, *W* Weak, *C* Contaminated.

TABLE II. γ-ray energies, intensities, and angular distribution coefficients measured using the ^{141}Pr(^{14}N, $4n$)^{151}Dy reaction. The table also gives the deduced level energies, branching ratios, probable multipolarities, and spin assignments.

E_{level}(keV)	E_γ(keV)	I_γ [a]	Br(%)	a_2(%)	a_4(%)	Multipolarity	$J_i^\pi - J_f^\pi$
527.40 ± 0.10	527.40 ± 0.10	74	100	11 ± 4	−7 ± 4	λ=1	$\frac{9}{2}^- - \frac{7}{2}^-$
775.53 ± 0.15	775.53 ± 0.15	39	100 [b]	+13 ± 2	−2 ± 2	2	$\frac{11}{2} - \frac{7}{2}$
968.53 ± 0.18	193.00 ± 0.10	3	100 [c]	*	*	(1)	$\frac{13}{2} - \frac{11}{2}$
1348.72 ± 0.11	573.2 ± 0.5	5	7 ± 1 [d]	*	*	(1)	$\frac{13}{2} - \frac{11}{2}$
	821.32 ± 0.05	68	93 ± 1	+12 ± 2	−4 ± 2	2	$\frac{13}{2} - \frac{9}{2}$
1511.08 ± 0.12	542.50 ± 0.10	3	9 ± 1	−5 ± 3	0 ± 5	1	$\frac{15}{2} - \frac{13}{2}$
	735.59 ± 0.05	29	91 ± 1	+9 ± 4	−3 ± 5	2	$\frac{15}{2} - \frac{11}{2}$
1918.54 ± 0.10	407.40 ± 0.10	32	30 ± 1	−14 ± 3	−2 ± 3	1	$\frac{17}{2} - \frac{15}{2}$
	569.88 ± 0.05	74	70 ± 1	+10 ± 2	−1 ± 4	2	$\frac{17}{2} - \frac{13}{2}$
2262.98 ± 0.11	344.44 ± 0.04	100	100	+13 ± 1	−5 ± 2	2	$\frac{21}{2} - \frac{17}{2}$
2911.62 ± 0.12	648.64 ± 0.05	99	100	+13 ± 1	−3 ± 2	2	$\frac{25}{2} - \frac{21}{2}$
2958.5 ± 0.2	46.9	*	* [e]	*	*	1	$\frac{27}{2} - \frac{25}{2}$
3428.4 ± 0.2	469.91 ± 0.12	16	100	−17 ± 4	0 ± 4	1	$\frac{29}{2} - \frac{27}{2}$
3733.9 ± 0.2	775.38 ± 0.15	72	100 [b]	+18 ± 1	3 ± 1	2	$\frac{31}{2} - \frac{27}{2}$
4306.3 ± 0.2	572.5 ± 0.5	7	70 ± 6 [d]	*	*	(1)	$\frac{33}{2} - \frac{31}{2}$
	877.79 ± 0.16	3	30 ± 6	+8 ± 4	−5 ± 5	(2)	$\frac{33}{2} - \frac{29}{2}$
4387.3 ± 0.2	653.37 ± 0.06	65	100	15 ± 1	−2 ± 1	2	$\frac{35}{2} - \frac{31}{2}$
4741.5 ± 0.2	354.28 ± 0.07	48	82 ± 1	−15 ± 3	+4 ± 4	1	$\frac{37}{2} - \frac{35}{2}$
	435.16 ± 0.13	11	18 ± 1	+18 ± 5	−10 ± 5	2	$\frac{37}{2} - \frac{33}{2}$
4903.8 ± 0.2	162.32 ± 0.05	59	100	+12 ± 2	−4 ± 2	2	$\frac{41}{2} - \frac{37}{2}$
5742.8 ± 0.2	839.02 ± 0.10	32	100	−8 ± 3	+3 ± 5	1	$(\frac{43}{2}) - (\frac{41}{2})$
5767.8 ± 0.3	25.0	*	* [e]	*	*	1	$(\frac{45}{2}) - (\frac{43}{2})$
6032.1 ± 0.3	264.29 ± 0.08	25	100	+9 ± 3	−4 ± 3	2	$(\frac{49}{2}) - (\frac{45}{2})$
6214.2 ± 0.3	182.07 ± 0.09	10	100	−14 ± 9	+9 ± 10	1	$(\frac{51}{2}) - (\frac{49}{2})$
7219.7 ± 0.4	1005.5 ± 0.2	7	100	−47 ± 15	+12 ± 16	1	$(\frac{59}{2}) - (\frac{51}{2})$

[a] The errors in intensity are ±1% or 1 unit whichever is largest.
[b] The analysis of the 775-keV doublet is discussed in the text.
[c] The 193-keV transition is obscured in the singles spectra. The dipole assignment is from parallel decays.
[d] The 573-keV doublet could not be resolved, but had $a_2 = -14 \pm 1\%$, $a_4 = -2 \pm 3\%$ indicating both decays are dipole in nature.
[e] Data on these totally converted transitions are from Piiparinen *et al.* (Ref. 10).

the reaction cross sections using the evaporation code ALICE[16] is also shown in Fig. 4(a) and can be seen to reproduce the maximum of each evaporation channel but overestimates the rapid decrease in cross section above the peak bombarding energy. Similar results to these have been reported for the ^{142}Nd(^{14}N, xn) reaction by Schmidt-Ott *et al.*[7] The evaporation of charged particles was predicted to be a factor of 10 weaker than neutron evaporation and no experimental evidence for prompt terbium γ rays was found.

The relative yield of ^{151}Dy transitions normalized to the 527-keV ground state decay was found to be unusual, as shown in Fig. 4(b). All low-lying transitions were found to have similar yield curves, while above 3 MeV excitation transitions were found to rise steeply with incident beam energy. The relative amount of prompt and delayed feeding changed rapidly with beam energy giving irregular curves so these data were not used for construction of the decay scheme or in spin assignments.

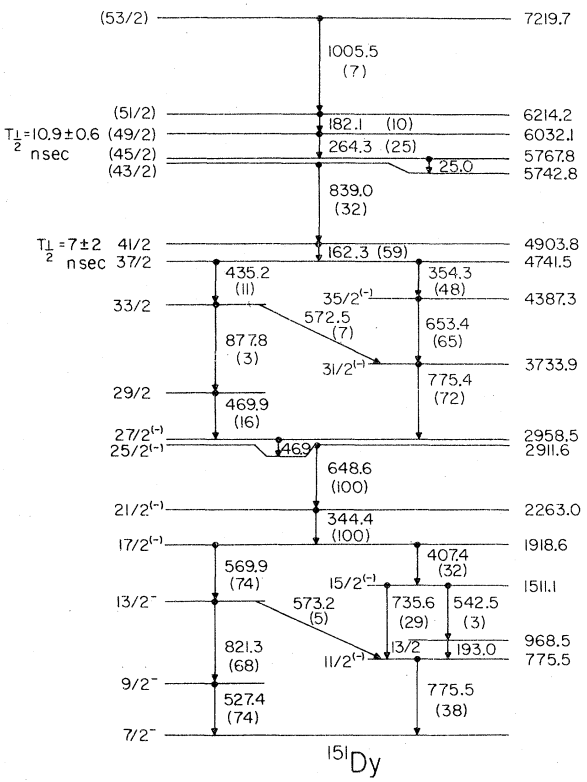

FIG. 3. The decay scheme of ^{151}Dy constructed from the data collected in this work. Spin assignments are firm up to the first isomer at 4904 keV and tentative above this point. The figures in parentheses indicate the intensity of the γ-ray transition in the 75-MeV ^{14}N+^{141}Pr in-beam experiment.

The construction of the decay scheme from the coincidence data presented some difficulties. Although much of the major decay cascade was forked, providing two parallel chains of γ coincidences, it was found that the intensity of the lower transitions could be almost entirely accounted for by cascade feeding, and so the relative ordering of the transitions in their cascades was difficult using the present data. The 527.4-keV $\frac{9}{2}^- - \frac{7}{2}^-$ transition was known to be a ground state decay.[7] The existence of two nearly degenerate 573-keV crossover transitions and the relative ordering of the 570- and 821-keV transitions were established by comparing the relative yields of 573-keV radiation in coincidence spectra gated by the 775-, 649-, and 344-keV lines. The 775 keV is a doublet. If two 573-keV transitions exist then since both feed levels deexciting by 775 keV the coincidence spectra for 775 keV will show enhanced 573 keV relative to coincidence spectra for the 640-keV and 344-keV line. This was found to be the case. Further evidence for this ordering was obtained from yields of 573-keV radiation in coincidence spectra gated by the 570- and 821-keV lines. The parallel decays from the 1918.5-keV level were difficult to order as the 775-keV line was found to be part of a closely spaced doublet and the 193-keV transition was obscured in the singles spectrum by a γ ray excited by reaction on the Ta target backing. However, by using the coincidence data it was possible to extract the relative strengths of the two members of the 775-keV doublet and to estimate the intensity of the 193-keV transition. This analysis indicated the intensities of the members of the 407-, 736-, 775-keV decay fork were very nearly equal, but suggested an ordering which was consistent with those reported by Fleissner[9] and Piiparinen.[10]

It was noted that a 344.4-keV line was present in radioactivity data collected after the completion of the experiment. This transition occurs in the β^+ decay chain from ^{152}Dy which was produced via the ^{141}Pr(^{14}N, $3n$)^{152}Dy reaction. A subtraction of 10± 2 in the intensity of the ^{151}Dy line was needed to correct for this. The construction of the higher-lying level scheme was relatively straightforward, as the decay cascade again forked and the intensity of transitions decreased with increasing excitation energy. However, these data were not sensitive to highly converted low energy transitions of $E_\gamma < 60$ keV. Piiparin *et al.*[10] studied conversion electrons and found evidence for two further levels at 2911.6 keV and 5742.8 keV de-exciting by an $M1$ decay of 46.9 keV and a $\lambda = 1$ decay of 25.0 keV, which have been included in the data shown in Fig. 3. The highest-lying level observed in the 75-MeV γ-γ data sorted with a 20-ns wide coincidence time requirement was the 6032-keV level. Resorting the data with a more relaxed coincidence time requirement of 200 ns gave clear evidence of 1005.5-keV and 182.1-keV transitions above this with nearly equal intensities. The observed γ intensities were corrected for internal conversion using the tables of Rösel *et al.*[15] These corrections were only appreciable for the 162- and 182-keV decays. The 162-keV transition can only be an $E2$ decay on the grounds of its half-life of 7± 2 ns and so correction for internal conversion is straightforward, requiring a 34% correction. However, the 182-keV decay may be $E1$ or $M1$; an $E1$ decay would require a correction of 6%, giving this transition and the 1005-keV decay very similar intensities making the ordering of these decays ambiguous, while an $M1$ decay would require a correction of 32% which places the 182-keV transition clearly lower in excitation than the 1005-keV decay. The decay scheme resulting

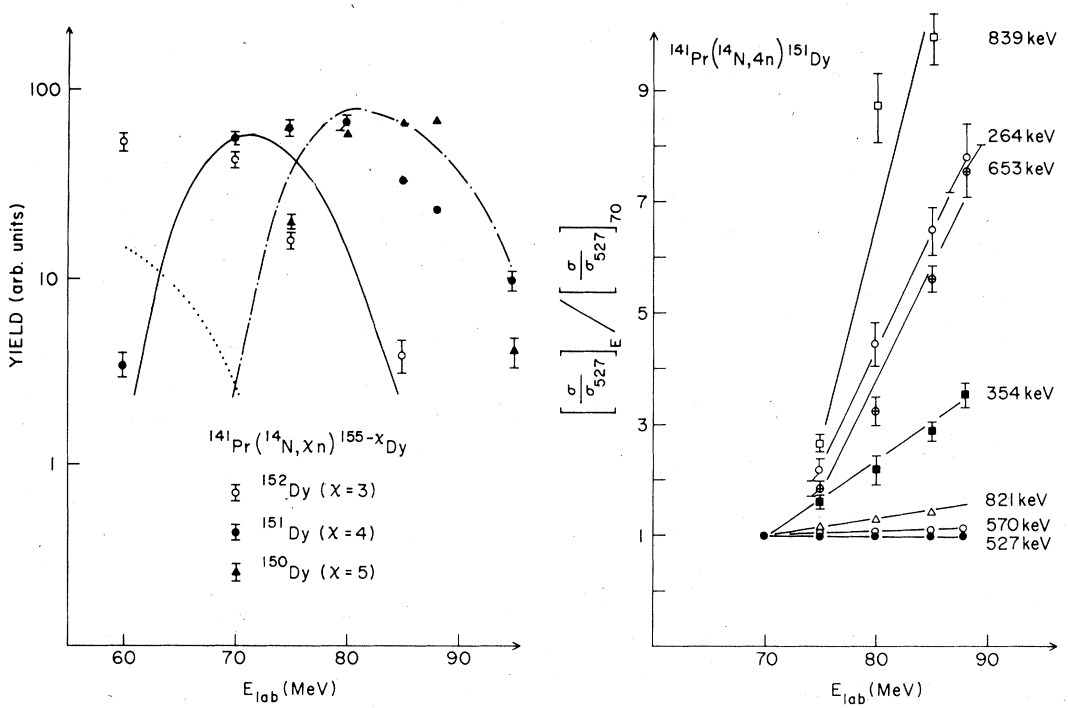

FIG. 4. Excitation function data collected in the ^{141}Pr+^{14}N study. (a) illustrates the relative yield from 3, 4, and 5 neutron emission compared with the predictions of the evaporation code ALICE, with ··· ^{152}Dy, ---- ^{151}Dy, and —·—·—·— ^{150}Dy. (b) illustrates the relative yield of some transitions in ^{151}Dy normalized to keep the 527-keV $\frac{9}{2}^- \rightarrow \frac{7}{2}^-$ ground state decay constant in intensity.

from the present work is shown in Fig. 3. The intensities shown in Fig. 3 and listed in Table II include the correction for internal conversion. Two additional dipole transitions not shown in Fig. 3 were found with energies 277.4 and 271.6 keV. The former decays to either the 2912- or 2958-keV level, and the latter decays to either the 5743- or 5768-keV level.

It is notable that the side feeding into the 6032- and 4904-keV isomers is appreciably larger than the side feeding into the other yrast states. In addition, the side feeding is small into the states below 4 MeV in excitation energy. This is reflected in the excitation functions shown in Fig. 4(b) where the data are normalized to make the yield of the 527-keV ground state decay constant with varying beam energy. It can be seen that the low-lying levels (which are populated mainly by cascade feeding) have nearly the same relative yield, independent of spin or excitation, while higher-lying levels (populated more directly) show rapidly increasing intensity above the point at which they are first observed.

The presence of isomers in the γ decay allows time for dealignment of the initial magnetic substate distribution due to hyperfine relaxation. This effect, together with the target ground state spin of $J=\frac{5}{2}$ and projectile spin of $J=1$ for the ^{141}Pr(^{14}N, xn) reaction, causes a reduction in the anisotropy of the γ-ray angular distributions. Using the parametrization of Yamazaki[17] to describe the alignment, and studying the transitions which appeared to be quadrupole in nature, it was found that the alignment parameter α_2 varied smoothly from $\alpha_2 \approx 0.2$ for the lower-lying states to $\alpha_2 \approx 0.5$ for the upper states. Transitions which were populated strongly from the isomers showed more attenuated alignment than would be expected for this trend with $\alpha_2 \approx 0.3$ for the 7 ns isomer and $\alpha_2 \approx 0.25$ for the 11 ns isomer.

The spin assignments shown in Fig. 3 are based on assignment $\Delta J = 2$ for transitions with $a_2 > 0$, $a_4 < 0$, and $\Delta J = 1$ for transitions with $a_2 < 0$, while assuming that spin increases with increasing excitation energy. In addition, the 46.9- and 25.0-keV transitions have been assigned $\Delta J = 1$ from conversion electron intensities. Although these assignments are not rigorous, with highly mixed and $J \rightarrow J$ transitions providing possible exceptions, they are supported by the fact that the stretched γ-ray decay along (and near) the yrast line is the dominant mode of de-excitation following heavy-ion induced reactions. Furthermore, the assignments made in ^{151}Dy involve

parallel decays which provide independent information on level spins. Consequently the assignments of spins up to the first isomer $J=\frac{41}{2}$ are considered firm, with more tentative assignments to higher-lying levels which de-excite through a single γ-ray cascade. Using the alignment parameters deduced for the quadrupole transitions, the angular distribution data indicate that the degree of mixing in the $\Delta J=1$ transitions is small, with a mixing ratio of $|\delta|<0.1$ in all cases except for the highly anisotropic 1005-keV transition where $(0.1<\delta<0.5)$.

Two transitions required special analysis. The 775-keV doublet was split into two components by subtracting from the combined angular distribution data the distribution of the lower quadrupole transition, using the average alignment for low-lying decays and relative intensities from the coincidence data. Similarly the 344-keV transition required the subtraction of an isotropic component due to a radioactive decay of the same energy. A compilation of the present results for ^{151}Dy is shown in Table II.

The time distributions of the γ radiation collected during the pulsed beam experiment were used to determine the lifetimes of the isomers. The 264-keV transition from the direct decay of the 6032-keV isomer, which could be analyzed by both the slope and the centroid shift methods since there was no prompt component in the time spectrum, gave half-lives of 10.7 ± 1.0 ns and 10.9 ± 0.6 ns, respectively, for the two techniques. These values agree with the half-life derived from the $^{32}S+^{122}Sn$ reaction data. The presence of the 4904-keV isomer resulted in the low-lying transitions giving an effective $\tau_{1/2}=15.3\pm0.6$ ns similar to the situation with the $^{32}S+^{122}Sn$ reaction data. These time spectra for low-lying γ rays were fitted to a two-component decay curve, resulting in a half-life for the lower isomer of 7 ± 2 ns.

Examination of the time relationships between pairs of γ rays observed in the 75-MeV direct current experiment allowed a confirmation of these results and permitted an upper limit to be set on the half-lives of other levels. The data were sorted to project the time spectrum measured between the occurrence of the strong 344-keV line in one detector and the other ^{151}Dy lines in the other. The results of this analysis can be seen in Fig. 5. The position of the centroid of each time distribution is dominated by an energy-dependent time walk, but in addition it is clear that there is a significantly larger time difference between the 182- and 1005-keV transitions and the lower-lying γ rays "prompt" with the 344-keV decay. The 264- and 839-keV transitions show an

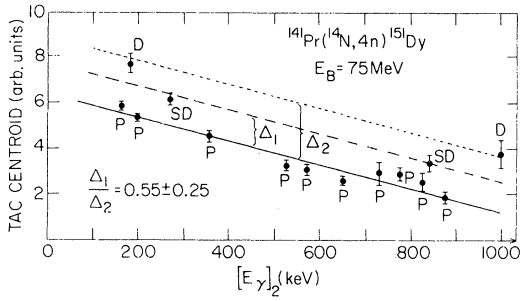

FIG. 5. An illustration of the timing relationships between various γ rays in one γ detector and the 344-keV decay in the other during the $^{141}Pr+^{14}N$ γ-γ coincidence experiment. While the time response is dominated by an energy-dependent walk, it is clear that there is a significant time difference between the emission of the 182- and 1005-keV γ rays from above the isomers and the 344-keV delay. Transitions of 264 and 839 keV show an intermediate delay allowing the confirmation of the half-life of the lower isomer as $\tau_{1/2}=7\pm2$ ns.

intermediate time difference. The scatter of points about the line corresponding to the prompt transitions gives a standard deviation of $\sigma=1.5$ ns, and all points lie within the 3σ value of 4.5 ns, which is considered to be a safe upper limit for the lifetime of any other of the low-lying levels.

Reduced electromagnetic transition strengths can be derived from the lifetime data for the isomers, and other limits to the electromagnetic strengths can be derived from the upper limit of the lifetimes of the other states. In many cases these rather convincingly fix the parity change in the transition. For example, both of the isomers decay by $E2$ transitions because $M2$ decays would require transition strengths in excess of 70 Weisskopf units (W.u.). The 264-keV decay of the upper isomer has a strength $B(E2)=0.77\pm0.04$ W.u. while the lower isomer has a 162-keV decay strength of $B(E2)=10\pm3$ W.u. The upper limit of 4.5 ns of the half-lives of the other states requires that the 344-, 435-, 570-, 648-, and 653-keV transitions, de-exciting the $\frac{21}{2}$, $\frac{37}{2}$, $\frac{17}{2}$, $\frac{25}{2}$, and $\frac{35}{2}$ states, respectively, almost certainly[18] must decay by $E2$ transitions because the alternative $M2$ transition strength would exceed 1.0 W.u. The 775.5-, 736-, 821-, and 775.4-keV transitions, de-exciting the $\frac{11}{2}$, $\frac{15}{2}$, $\frac{13}{2}$, and $\frac{31}{2}$ states, respectively, also have a high probability that they are $E2$ transitions, since the alternative $B(M2)$ would exceed 0.5 W.u., which is unlikely. Thus the members of the most strongly excited cascade sequence up to the 4387.3-keV level are likely to have negative parity.

Piiparinen *et al.*[10] note it is difficult to determine the ordering of the 264-keV and 25-keV decays.

If the isomer were de-excited by the 25-keV $\lambda = 1$ transition, instead of the 264-keV $E2$ transition, the transition strength for the isomeric decay would have a value of $B(E1) = 6.1 \times 10^{-4}$ W.u. or $B(M1) = 8.1 \times 10^{-3}$ W.u., depending on the type of transition. These are still not untypical of single-particle transitions. However, the data from the pulsed beam experiment show that the 264-keV transition has no "prompt" component which suggests that this is the isomeric decay.

The result of resorting the 80-MeV pulsed beam data with a prompt-delayed γ-γ coincidence requirement with respect to the beam considerably enhanced the relative strength of decays from states above the isomers. The 182- and 1005-keV transitions became prominent together with a series of lines not previously seen in the coincidence data and only weakly in singles. The energies and intensities of these lines are shown in Table III, and the transitions were found to have yield curves similar to those of other high-lying ^{151}Dy transitions. Unfortunately, coincidence statistics were too poor to allow gating on these lines individually in order to construct the exact pattern of γ decay above the $J = \frac{53}{2}$ state at 7220 keV.

IV. DISCUSSION

A. General features

Plots of the excitation energy of the yrast sequence versus $J(J+1)$ for $^{151}_{65}Tb_{86}$,[21] $^{151}_{66}Dy_{85}$, and $^{152}_{66}Dy_{86}$ are shown in Fig. 6. In all three nuclei the yrast sequence exhibits an irregular dependence on excitation energy characteristic of an independent particle structure. This contrasts with the smooth behavior of collective rotation which is such a ubiquitous feature in rare-earth nuclei. The half-lives and corresponding $B(E2)$ values in Weisskopf units of isomeric $E2$ transitions in ^{151}Dy and ^{152}Dy are summarized in Table IV. These $E2$ transition strengths are comparable with single-particle estimates, that is, these $E2$ transitions are retarded by between one and two orders of magnitude relative to typical collective rotational values.

TABLE III. γ rays showing strong enchancement in a prompt-delayed sort of γ-γ coincidence data following the ^{141}Pr(^{14}N, $4n$)^{151}Dy pulsed beam experiment. The data are normalized such that the intensity of the 264-keV transition is 100 units.

E_γ (keV)	$I_{(\gamma)}$
418.8 ± 0.7	15 ± 2
1084.8 ± 1.2	13 ± 3
958.7 ± 0.7	11 ± 2
991.2 ± 0.7	10 ± 2
625.6 ± 0.5	10 ± 2
1142.2 ± 1.5	7 ± 3
377.6 ± 0.5	6 ± 3

It can be seen in Fig. 6 that the excitation energies of the yrast sequence in ^{151}Tb, ^{151}Dy, and ^{152}Dy all scatter closely about a straight line for $J(J+1) > 250$. The slopes of these lines yield effective moments of inertia of $2I/\hbar^2 = 117$ MeV^{-1}, 138 MeV^{-1}, and 142 MeV^{-1}, the latter being 18% and 20% larger than the rigid sphere values, respectively. The values extracted depend sensitively on observing all transitions in the yrast sequence, most notably low-energy transitions as the 25- and 47-keV transitions. Failure to observe one such low-energy transition with multipolarity 1 at spin ~$20\hbar$ leads to a 10% error in the effective moment extracted from such plots. Noting that considerable evidence exists to regard $^{146}_{64}Gd_{82}$ as a doubly magic nucleus,[22] the observed I_{eff}'s for ^{151}Dy and ^{152}Dy display a behavior similar to that observed for nuclei near the $N = 126$ closed shell.[23] In the latter case moments were found to exhibit a smooth increase above the spherical value for increasing number of valence nucleons.

Although the moment of inertia for collective rotation about a symmetry axis has no meaning for quantal systems, it was shown by Bohr and Mottelson[19] that, on the basis of the Fermi-gas approximation, the locus of the yrast sequence for alignment of single-particle orbits along a symmetry axis corresponds to an effective moment of inertia equal to that of a rigid body with the same density distribution as the nucleus. The Bohr and Mottelson estimate of the effective moment of inertia is proportional to the density of single-particle orbits around the Fermi level. This density is assumed to be uniformly distributed in the Fermi-gas approximation, that is, shell effects are not considered. If the Fermi level is close to a shell closure, then the density of single-particle orbits, and hence the effective moment of inertia, will be smaller than the Fermi-gas estimate (rigid body value). This effect is demonstrated in ^{212}Rn where the effective moment of inertia for $20 \leq J \leq 30$ is observed[20] to be 80% of the rigid body value. Conversely one may expect the effective moment of inertia to exceed the Fermi-gas estimate well away from shell closure as is observed in these data and ^{152}Dy.

Calculations of the yrast levels for nuclei near the $N = 82$ shell closure have been made by several authors[24-27] and isomerism widely predicted. These isomers arise when members of the yrast sequence are depressed relative to the trend along

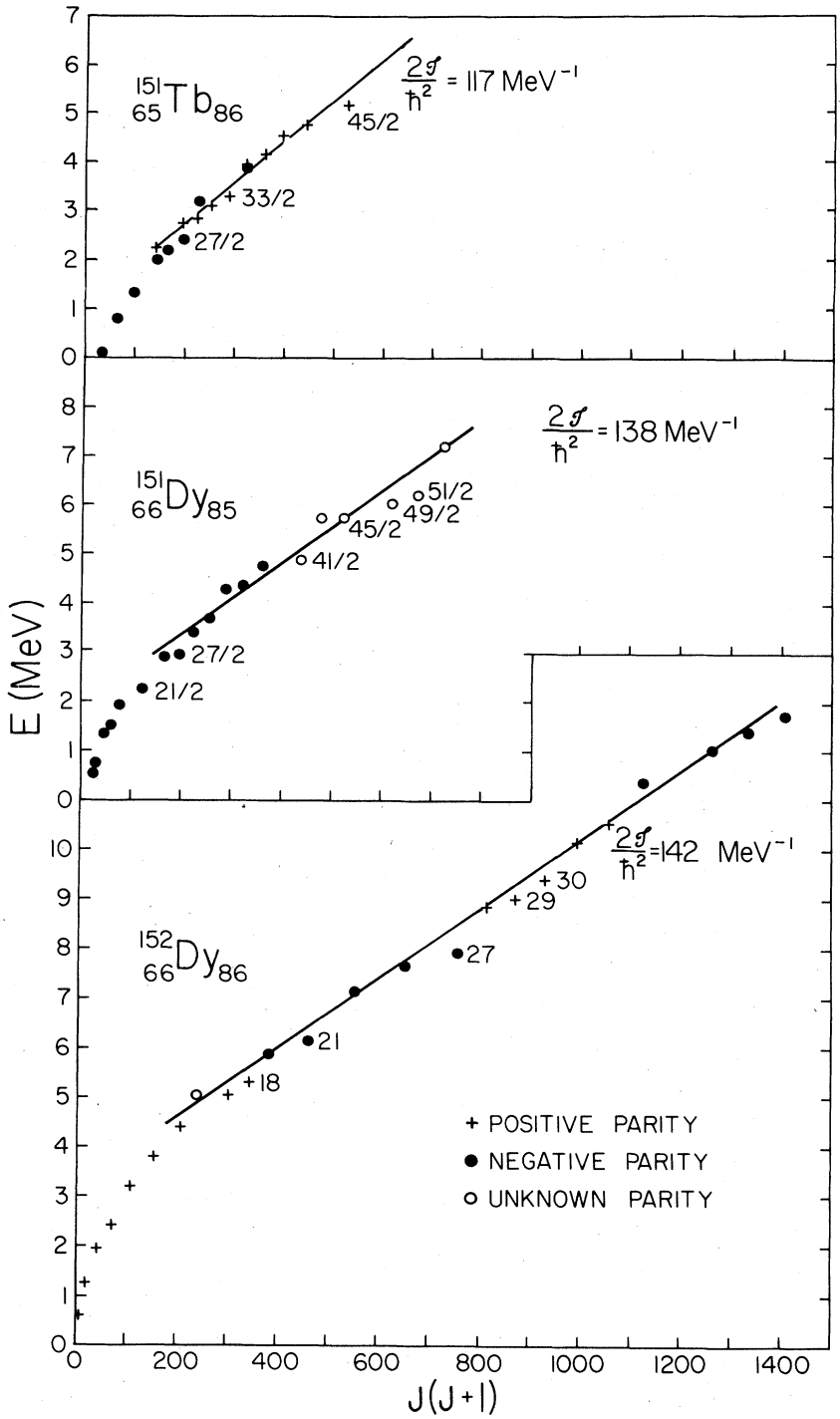

FIG. 6. A plot of excitation energy against $J(J+1)$ for levels in ^{151}Tb, ^{151}Dy, and ^{152}Dy. Data are taken from Ref. 21, the present work, and Ref. 5, respectively. The irregular nature of the yrast line is clearly seen. Also shown are straight lines with effective moments of inertia of 117 MeV^{-1}, 138 MeV^{-1}, and 142 MeV^{-1} for ^{151}Tb, ^{151}Dy, and ^{152}Dy.

the yrast line. If this depression is large and the level falls below the next lower state in the yrast cascade, then the decay must be by a high multipolarity transition, which is unfavorably slow. Alternatively a lesser depression to a position slightly above the next lowest member results in a low energy γ-ray transition, which is also long-lived.

TABLE IV. $E2$ isomeric transitions in ^{151}Dy and ^{152}Dy.

Nucleus	Suggested or experimental initial and final I^π	Half-life or partial half-life (ns)	Energy of isomeric transition (keV)	$B(E2)$ in W.u.
^{151}Dy	$\frac{41}{2}^{(-)} \rightarrow \frac{37}{2}^{(-)}$	7 ± 2	162	10 ± 3
^{151}Dy	$(\frac{49}{2}) \rightarrow (\frac{45}{2})$	10.9 ± 0.6	264	0.77 ± 0.04
^{152}Dy	$17^+ \rightarrow 15^+$	60	$54 \geq \Delta \geq 12$	$12-15$[a]
			$\Delta < 12$	>15[a]
^{152}Dy	$21^- \rightarrow 19^-$	10 ± 1	262	0.88 ± 0.06
^{152}Dy	$27^- \rightarrow 25^-$	1.5 ± 0.2	220	13 ± 2
^{152}Dy	$30^+ \rightarrow 28^+$	>0.07	550	<6
^{152}Dy	$31^+ \rightarrow 29^+$	0.038 ± 0.012	1114	0.26 ± 0.10
^{152}Dy	$32^+ \rightarrow 30^+$	0.059 ± 0.006	1143	<0.4

The experimental data are based on the present paper for ^{151}Dy and Refs. 3 and 5 for ^{152}Dy.

[a] $E2$ multipolarity assumed on the basis of theoretical considerations and the suggestion of Ref. 5.

B. Spherical shell model configurations

Grover[27] performed combinatorical calculations based on a spherical shell model of noninteracting fermions, except that the pairing correlations were taken into account in the usual way. This very simple shell model calculation allowed Grover to calculate the yrast sequence and the adjacent few levels to $J = 70\ \hbar$.

This model calculation predicts an undulating energy dependence of the yrast sequence and even suggests a 27^- isomer would occur in ^{152}Dy in agreement with experiment. However, this agreement is probably fortuitous since the other suggested isomers do not agree with the experiment. For $J \geq 18$ the average slope of the yrast sequence corresponds to an effective moment of inertia 1.5 times the rigid body value and 1.34 times the experimental value. This indicates that the level density of single-particle orbits at the Fermi level in this calculation is too high and that a large effective moment of inertial need not imply large deformation.

No detailed spherical shell model calculations are available for ^{151}Dy. The major configurations involved in the yrast sequence can only be inferred from a simple single-particle model and data on neighboring nuclei. In several respects $^{146}_{64}Gd_{82}$ behaves like a doubly magic nucleus.[22] Assuming this is a doubly closed core, then the $(\nu f_{7/2})^3$ configuration probably accounts for a major part of the wave functions of the $J = \frac{7}{2}^-$ to $\frac{15}{2}^-$ yrast states in $^{151}_{66}Dy_{85}$. The well-known $M1$ forbiddenness between j^n configurations could partially account for the parallel branches in the decay of these states.[28] In addition, the $(\nu f_{7/2}^2 \otimes \nu h_{9/2})_J$ configuration will contribute to this parallel branching and could account for states up to $J^\pi = \frac{21}{2}^-$ at 2263 MeV. Data on the $(\pi h_{11/2})^2$ nucleus ^{148}Dy (Ref. 29) indicate that above ~2.9 MeV the $(\pi h_{11/2}^2)_{J=0}$ pair can be broken to form $(\pi h_{11/2}^2)_{J=10}$ which will couple with $(\nu f_{7/2}^3)$ to form states up to $J^\pi = \frac{35}{2}^-$ and with $(\nu f_{7/2}^2 \otimes \nu h_{9/2})$ to form states up to $\frac{41}{2}^-$. The coupling of $(\nu h_{11/2}^2)_{J=10}$ and the $(\nu f_{7/2} \otimes \nu h_{9/2} \otimes \nu i_{13/2})$ configuration will produce states up to spin $\frac{49}{2}^+$.

It is noted that the decay scheme above the $\frac{27}{2}^-$ state, up to the $\frac{41}{2}^-$ state, is remarkably similar to that below the $\frac{27}{2}^-$ state, from the $\frac{7}{2}^-$ ground state up to the $\frac{21}{2}^-$ state. In both these subsets of the decay scheme a similar forking behavior is observed, nearly degenerate (572.5-vs 573-keV) crossover transitions are found, spin sequences correspond, and corresponding decays have similar transition energies. Such a behavior strongly suggests weak coupling of the same excited neutron configurations to a $(\pi h_{11/2}^2)_{J=0}$ proton core for the lower part and to a $(\pi h_{11/2}^2)_{J=10}$ core for the upper part.

The short-range attractive residual two-body interaction produces especially large binding for maximally aligned neutron-proton (or $T = 0$) configurations due to maximization of overlap of nucleonic wave functions (the MONA effect[30]). Thus the maximally aligned neutron-proton configurations of high j orbitals should be somewhat depressed in excitation energy, and this could explain why certain high-spin states lie below the lines drawn through the average of the yrast sequences shown in Fig. 6 and hence produce isomers at $\frac{41}{2}^-$ and $\frac{49}{2}^+$. Table V lists the maximum spin neutron-proton shell model configurations,

TABLE V. The spherical shell model and aligned oblate spherical model configurations expected to dominate the structure of high spin yrast states depressed in excitation energy relative to the neighboring yrast states.

Nucleus	J^π	(a) Spherical shell model n	(a) Spherical shell model p	(b) Oblate spheroidal model n	(b) Oblate spheroidal model p
$^{151}_{65}Tb_{86}$	$\frac{33}{2}^+$	$[h_{9/2}i_{13/2}]_{11^-}$	$[h_{11/2}]_{11/2^-}$	11^-	$(h_{11/2})_{11/2^-}$
	$\frac{45}{2}^+$	$[(f_{7/2}{}^2)_6 h_{9/2}i_{13/2}]_{17^-}$	$[h_{11/2}]_{11/2^-}$	17^-	$(h_{11/2})_{11/2^-}$
	$\frac{51}{2}^-$	$[h_{9/2}f_{7/2}(i_{13/2}{}^2)_{12}]_{20^+}$	$[h_{11/2}]_{11/2^-}$	20^+	$(h_{11/2})_{11/2^-}$
$^{151}_{66}Dy_{85}$	$\frac{35}{2}^-$	$[f_{7/2}{}^3]_{15/2^-}$	$[h_{11/2}{}^2]_{10^+}$		
	$\frac{39}{2}^-$			$\frac{29}{2}^+$	5
	$\frac{41}{2}^-$	$[(f_{7/2}{}^2)_6 h_{9/2}]_{21/2^-}$	$[h_{11/2}{}^2]_{10^+}$		
	$\frac{45}{2}^+$	$[(f_{7/2}{}^2)_6 i_{13/2}]_{25/2^+}$	$[h_{11/2}{}^2]_{10^+}$		
	$\frac{49}{2}^+$	$[f_{7/2}h_{9/2}i_{13/2}]_{29/2^+}$	$[h_{11/2}{}^2]_{10^+}$	$\frac{29}{2}^+$	10^+
$^{152}_{66}Dy_{86}$	18^+	$[h_{9/2}{}^2]_{8^+}$	$[h_{11/2}{}^2]_{10^+}$		
	21^-	$[h_{9/2}i_{13/2}]_{11^-}$	$[h_{11/2}{}^2]_{10^+}$	11^-	10^+
	27^-	$[(f_{7/2}{}^2)_6 h_{9/2}i_{13/2}]_{17^-}$	$[h_{11/2}{}^2]_{10^+}$	17^-	10^+
	30^+	$[h_{9/2}f_{7/2}(i_{13/2}{}^2)_{12}]_{20^+}$	$[h_{11/2}{}^2]_{10^+}$	20^+	10^+

based on a $^{146}_{64}Gd_{82}$ closed core which should be depressed in energy for the high-spin states in ^{151}Tb, ^{151}Dy, and ^{152}Dy. These configurations nicely reproduce the parity and spin of depressed states in ^{151}Tb and ^{152}Dy and the $\frac{41}{2}$ and $\frac{49}{2}$ states in ^{151}Dy.

C. Oblate spheroidal multiparticle configurations

Calculations of multiparticle configurations having the symmetry and rotation axes aligned are most easily performed, assuming the cranking of an oblate spheroidal single-particle potential. Despite use of a deformed basis, no collective rotation can take place around a symmetry axis and thus the yrast states of the oblate structure are of single-particle character. Calculations using the model by Andersson *et al.*[24,25] assumed an oblate modified oscillator single-particle potential with $\beta_2 = 0.1$ and included pairing. The similar calculations of Cerkaski *et al.*[26] assumed an axially symmetric oblate Woods-Saxon single-particle potential with $\beta_2 = -0.16$ and $\beta_4 = 0.03$. We have chosen to compare the data with the calculations using a Woods-Saxon potential.[26]

For 66 protons the 0^+ ground state assumes a filled $1g_{7/2}$ and $2d_{5/2}$ orbits with the extra two protons in the $[h_{11/2\,11/2}]$ orbits. Here the same notation $[l_j\Omega]$ as in Ref. 26 is used for describing the single-particle components of multiparticle configurations where l = orbital momentum and Ω = projection of the total angular momentum j on the symmetry axis. The lowest energy optimal proton configurations with respect to this ground state are

$$5^- = [d_{5/2\,-1/2}]^{-1}[h_{11/2\,9/2}],$$

$$10^+ = [h_{11/2\,11/2}][h_{11/2\,9/2}].$$

The neutron ground state for $N = 85$ has the three extra core neutrons in the $[f_{7/2\,7/2}]$ and $[h_{9/2\,7/2}]$ orbits. The lowest optimal configurations with respect to this ground state are

$$\tfrac{9}{2}^- = [h_{9/2\,9/2}],$$

$$\tfrac{29}{2}^+ = [f_{7/2\,7/2}][h_{9/2\,9/2}][i_{13/2\,13/2}].$$

The lowest optimal neutron configurations for $N = 86$ have spin 11^-, 17^-, and 20^+. The suggested structures of some high spin doubly optimal configurations in ^{151}Tb, ^{151}Dy, and ^{152}Dy are listed in Table V. It can be seen from Fig. 6 and Table V that the predicted optimal states are just the depressed states seen in ^{151}Tb and ^{152}Dy. In addition, the similarity of the spherical shell model and oblate spheroidal model descriptions is notable for these states.

For ^{151}Dy the relationships between the experimental data and the two types of calculation are not so clear. The oblate spheroidal models of Andersson and Cerkaski both predict a doubly optimal $J^\pi = \frac{39}{2}^-$ isomer, which is inconsistent with experiment and the spherical shell model

expectation. On the other hand, these calculations do not predict the observed $\frac{41}{2}$ isomer which is predicted by the spherical shell model. The predicted doubly optimal $\frac{49^+}{2}$ state agrees with experiment and is similar in structure to the $\frac{49^+}{2}$ shell model state.

It is noted that a successful detailed comparison of shell model and experimental results depends critically upon inclusion of the two low energy dipole transitions of 25 and 47 keV. Their omission leads to apparent contradiction between shell model and experimental results.

V. CONCLUSION

The yrast sequence of levels to spin $\frac{53}{2}$ and the low-lying level structure have been measured for ^{151}Dy. The yrast line does not display a rotational structure, but is irregular with an effective moment of inertia 1.18 times that of a rigid spherical ^{151}Dy nucleus for spins above $\frac{25}{2}$. Yrast isomers were found at J, E_x of $\frac{41}{2}$, 4903.9 keV and $\frac{49}{2}$, 6032.1 keV with lifetimes of $\tau_{1/2} = 7 \pm 2$ ns and 10.9 ± 0.6 ns, respectively. $B(E2)$ values extracted from the transitions de-exciting the isomers have values characteristic of single-particle transitions.

The nuclei ^{151}Tb and ^{151}Dy, with five nucleons outside a closed-shell ^{146}Gd core, and ^{152}Dy with six valence nucleons, have been found to have effective moments of inertia equal to (^{151}Tb) or exceeding the rigid sphere value (by 18% for ^{151}Dy and 20% for ^{152}Dy) for the high-spin portion of the yrast sequence. The latter values display a similar behavior to moments found for nuclei near the $N = 126$ shell closure,[23] in which case a smooth increase above the spherical value with increasing number of valence nucleons was found. The irregularity of the yrast line, the presence of isomers, and similarity of decay strengths all indicate a close relation in structure. A discussion of the structure of these isomers in terms of simple configurations in both a spherical shell model basis and an oblate spheroidal basis is successful for ^{151}Tb, ^{151}Dy, and ^{152}Dy.

The authors would like to thank Dr. T. L. Khoo, Dr. P. Kleinheinz, Dr. D. Horn, Dr. J. Dudek, Dr. Z. Szymanski, and Dr. R. K. Smither for useful discussion and communication of results prior to publication. G. R. Y. acknowledges support from Chaim Weizmann and Eugene Wigner Fellowships while R. L. and R. F. acknowledge support from the MIT UROP Program. This research was sponsored in part by a grant from the NSF (University of Rochester) and in part by the Division of Basic Energy Sciences, U. S. Department of Energy, under Contract No. W-7405-eng-26 with the Union Carbide Corporation (ORNL), under Contract No. EY-76-C-02-3069 (MIT), and under Contract No. EY-76-C-02-0016 (BNL).

---

*Permanent address: Institute of Experimental Physics, University of Warsaw, ul Hoza 69, 00-681 Warszawa, Poland.

†Present address: University of Liverpool, P. O. Box 147, Liverpool L69 3BX, United Kingdom.

[1]A. Bohr and B. R. Mottelson, Phys. Scr. 10A, 13 (1974).

[2]J. Pedersen *et al.*, Phys. Rev. Lett. 39, 990 (1977).

[3]T. L. Khoo, R. K. Smither, B. Haas, O. Haüsser, H. R. Andrews, D. Horn, and D. Ward, Phys. Rev. Lett. 41, 1027 (1978).

[4]J. F. W. Jansen, Z. Sujkowski, D. Chmielewska, F. B. Bruining, and R. J. de Meyer, KVI Annual Reports, Groningen, Holland, 1974, 1975 (unpublished), and Nucl. Phys. A321, 365 (1979).

[5]B. Haas, H. R. Andrews, O. Haüsser, D. Horn, J. F. Sharpey-Schafer, P. Taras, W. Trautmann, D. Ward, T. L. Khoo, and R. K. Smither, Phys. Lett. (to be published).

[6]J. C. Merdinger, F. A. Beck, T. Byrski, C. Gehringer, J. P. Vivien, E. Bozek, and J. Styczen, Phys. Rev. Lett. 42, 23 (1979).

[7]W. D. Schmidt-Ott, K. S. Toth, E. Newman, and C. R. Bingham, Phys. Rev. C 10, 296 (1974); K. S. Toth, C. R. Bingham, H. K. Carter, B. G. Ritchie, D. C. Sousa, and D. R. Zolnowski, Oak Ridge Annual Report No. ORNL 5025, 49, 1975 (unpublished) and private communication.

[8]C. J. Lister, G. R. Young, P. A. Butler, R. Ledoux, R. Fredieu, D. Cline, J. Srebrny, and D. Elmore, Bull. Am. Phys. Soc. 23, 944 (1978).

[9]J. G. Fleissner, E. G. Fink, and J. H. Mihelich, Bull. Am. Phys. Soc. 23, 627 (1978).

[10]M. Piiparinen, P. Kleinheinz, S. Lunardi, H. Backe, and J. Blomqvist, Z. Phys. 290, 337 (1979), and in Proceedings of the Symposium on High Spin Phenomena in Nuclei, Argonne, Illinois, 1979 (to be published).

[11]R. K. Smither, T. L. Koo, O. Haüser, H. R. Andrews, D. Horn, and D. Ward, Bull. Am. Phys. Soc. 23, 944 (1978).

[12]M. Piiparinen, L. Carlen, H. Ryde, S. A. Hjorth, A. Johnson, and Th. Lindblad, Phys. Scr. 17, 103 (1978).

[13]J. T. Routti and S. G. Prussin, Nucl. Instrum. Methods 72, 127 (1967).

[14]A. M. Stefanini, P. J. Daly, P. Kleinheinz, M. R. Maier, and R. Wagner, Nucl. Phys. A258, 34 (1976).

[15]F. Rösel, H. M. Fries, K. Alder, and H. C. Pauli, At. Data Nucl. Data Tables 21, 110 (1978).

[16]M. Blann and F. Plasil, USAEC Report No. C00-3494-10 (unpublished); M. Blann, Nucl. Phys. 80, 223

(1966).
[17]T. Yamazaki, Nucl. Data 3, 1 (1967).
[18]See, for example, Nucl. Data Sheets 24, No. 1, vi (1978).
[19]A. Bohr and B. R. Mottelson, *Nuclear Structure* (Benjamin, New York, 1975), Vol. 2, pp. 43 and 44, 72 ff, 80 ff.
[20]D. Horn, O. Haüsser, T. Faestermann, A. B. McDonald, T. K. Alexander, J. R. Beene, and C. J. Kerrlander, Phys. Rev. Lett. 39, 1387 (1977).
[21]P. Kennitz, L. Funke, F. Stary, E. Will, G. Winter, S. Elfstrom, S. A. Hjorth, A. Johnson, and Th. Lindblad, Nucl. Phys. A311, 11 (1978).
[22]P. Kleinheinz, S. Lunardi, M. Ogawa, and M. R. Maier, in *Proceedings of the International Conference on Nuclear Structure, Tokyo, 1977,* edited by T. Marumori (Physical Society of Japan, Tokyo, 1978), p. 864; Proceedings International Symposium on High-Spin States and Nuclear Structure, Dresden, 1977, Rossendorf Report No. ZIK-366, 1977, p. 25.
[23]D. Horn, O. Haüsser, B. Haas, T. K. Alexander, T. Faestermann, H. R. Andrews, and D. Ward, Nucl. Phys. A317, 520 (1979).
[24]C. G. Andersson and J. Krumlinde, Nucl. Phys. A291, 21 (1977).
[25]C. G. Andersson, G. Hellstrom, G. Leander, I. Ragnarsson, S. Åberg, J. Krumlinde, S. G. Nilsson, and Z. Szymanski, Nucl. Phys. A309, 141 (1978).
[26]M. Cerkaski, J. Dudek, P. Rozmej, and Z. Szymanski, Nucl. Phys. A315, 269 (1979).
[27]J. R. Grover, Phys. Rev. 157, 832 (1967).
[28]R. N. Horoshko, D. Cline, and P. M. S. Lesser, Nucl. Phys. A149, 562 (1970).
[29]P. J. Daly, P. Kleinheinz, R. Broda, A. M. Stefanini, and S. Lunardi, Z. Phys. A288, 103 (1978).
[30]A. Faessler, M. Ploszajczak, and K. R. S. Devi, Phys. Rev. Lett. 36, 1028 (1976).